A Density Functional Theory Study of the Mechanism of Free Radical Generation in the System Vanadate/PCA/H_2O_2

Rustam Z. Khaliullin,[†,‡] Alexis T. Bell,*[,†,§] and Martin Head-Gordon[†,‡]

Chemical Sciences Division, Lawrence Berkeley National Laboratory, Berkeley, California 94720, and Department of Chemistry and Department of Chemical Engineering, University of California, Berkeley, California 94720

Received: May 12, 2005; In Final Form: July 27, 2005

Experimental studies by Shul'pin and co-workers have shown that vanadate anions in combination with pyrazine-2-carboxylic acid (PCA ≡ pcaH) produce an exceptionally active complex that promotes the oxidation of alkanes and other organic molecules. Reaction of this complex with H_2O_2 releases HOO• free radicals and generates V(IV) species, which are capable of generating HO• radicals by reaction with additional H_2O_2. The oxidation of alkanes is initiated by reaction with the HO• radicals. The mechanism of hydrocarbon oxidation with vanadate/PCA/H_2O_2 catalyst has been studied using density functional theory. The proposed model reproduces the major experimental observations. It is found that a vanadium complex with one pca (PCA ≡ pcaH) and one H_2O_2 ligand is the precursor to the species responsible for HOO• generation. It is also found that species containing two pca ligands and an H_2O_2 molecule do not exist in the solution, in contradiction to previous interpretations of experimental observations. Calculated dependences of the oxidation rate on initial concentrations of PCA and H_2O_2 have characteristic maxima, the shapes of which are determined by the equilibrium concentration of the active species. Conversion of the precursors requires hydrogen transfer from H_2O_2 to a vanadyl group. Our calculations show that direct transfer has a higher barrier than pca-assisted indirect transfer. Indirect transfer occurs by migration of hydrogen from coordinated H_2O_2 to the oxygen of a pca ligand connected to the vanadium atom. The proposed mechanism demonstrates the important role of the cocatalyst in the reaction and explains why H_2O_2 complexes without pca are less active. Our work shows that the generation of HOO• radicals cannot occur via cleavage of a V−OOH bond in the complex formed directly from the precursors, as proposed before. The activation barrier for this process is too high. Instead, HOO• radicals are formed via a sequence of additional steps involving lower activation barriers. The new mechanism for free radical generation underestimates the observed rate of hexane oxidation by less than an order of magnitude; however, the calculated activation energy (67−81 kJ/mol) agrees well with that determined experimentally (63−80 kJ/mol).

Introduction

Vanadium-containing enzymes and homogeneous catalysts are known to promote the oxidation of various organic compounds by hydrogen peroxide and alkyl peroxides.[1] Shul'pin and co-workers have reported that vanadate cations in combination with pyrazine-2-carboxylic acid (PCA ≡ pcaH) produce a complex that is exceptionally active for promoting the oxidation of alkanes to alkyl peroxides, alcohols, and ketones, and the oxidation of alcohols to ketones and aldehydes.[2] What is particularly interesting about this system is that H_2O_2 plays the role of a promoter, whereas the true oxidant is O_2. On the basis of rate measurements, spectroscopic data, and the distribution of products formed, Shul'pin et al.[3] have proposed that the oxidation of alkanes involves the formation of HO• radicals via the mechanism shown in Figure 1. A vanadium complex containing one pca ligand (**I**) coordinates an H_2O_2 molecule to produce complex **II**. While complexes containing two pca ligands and one H_2O_2 ligand can readily form, they do not contribute to the reaction mechanism. **II** undergoes an intramolecular proton transfer from H_2O_2 to one of the V═O bonds in the complex, resulting in a new complex, **III**. Shul'pin et al.[3] propose that this process occurs indirectly via what they refer to as a "robot's arm mechanism", in which the proton transfer moves first to one of the N atoms of the pyrazine ring and then to the vanadyl group. The effectiveness of PCA as a cocatalyst in comparison with other amino acids (picolinic acid, imidazole-4,5-dicarboxylic, imidazole-4-carboxylic acid, and pyrazole-3,5-dicarboxylic acid) is attributed to the ability of PCA to facilitate the proton transfer step from H_2O_2 via the robot's arm mechanism. Once formed, **III** decomposes to produce HOO• radicals and a V^{IV} complex (**IV**). **IV** reacts with a second H_2O_2 molecule to generate a hydroxyl radical, which then attacks alkane molecules, RH, to produce alkyl radicals, R•. The latter species reacts with O_2 to form peroxyl radicals, ROO•, which then terminate to form alkyl hydroperoxides, the observed final product.

In the present study, density functional theory was used to investigate the energetics of free radical generation via the sequence of reactions proposed by Shul'pin et al.[3] Particular attention was focused on determining the composition of the active species from which free radicals are formed and to determine the elementary processes involved in the generation

* Corresponding author: bell@cchem.berkeley.edu.
† Lawrence Berkeley National Laboratory.
‡ Department of Chemistry, University of California.
§ Department of Chemical Engineering, University of California.

10.1021/jp058162a CCC: $30.25
Published on Web 09/07/2005

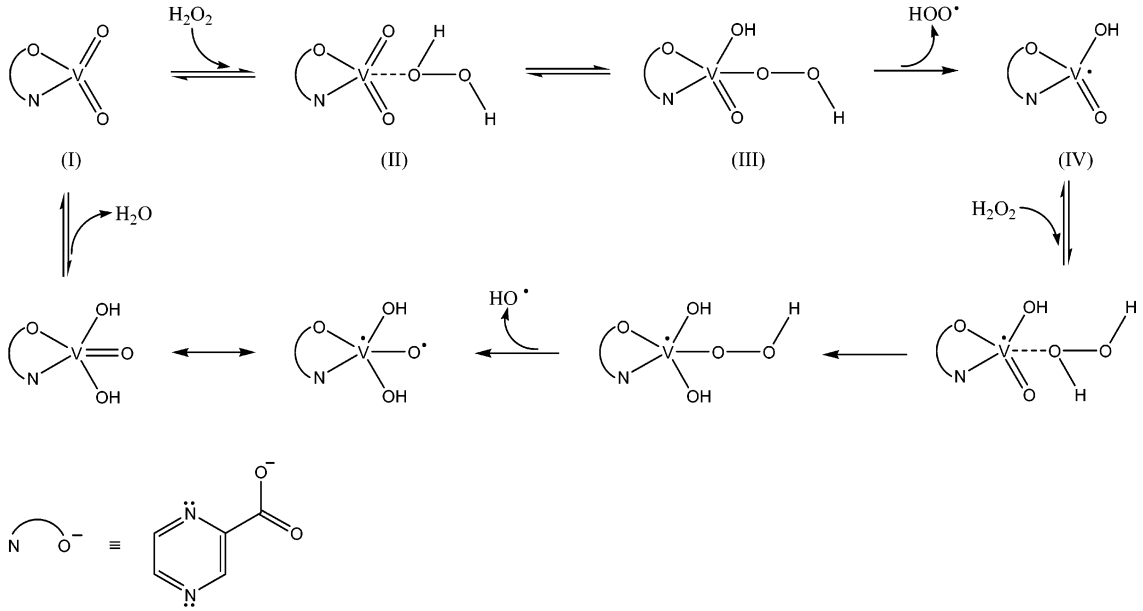

Figure 1. Proposed catalytic cycle for HOO• and HO• radical generation.

of HOO• radicals. The role of PCA in the transfer of protons from adsorbed H_2O_2 was examined in order to establish the importance of indirect proton transfer (i.e., the robot's arm mechanism) relative to direct proton transfer. Where possible, the results of our calculations were compared with the experimental observations reported by Shul'pin et al.[3]

Theoretical Approach

Figure 1 illustrates the structures that we have considered in this study. We have found that it is crucial to include solvent molecules in the coordination sphere of vanadium in order to obtain reasonable energetics for each of the elementary reactions. The inclusion of solvent also ensures that the coordination sphere of vanadium remains full. All reactions involving ions were treated as though only neutral species are involved. This approach avoids the need to account for solvation effects, which cannot be handled accurately without including the first shell of solvent molecules explicitly and thereby increasing the computational burden significantly. Thus, for example, reaction i involving negative ions is replaced by reaction ii in which each of the anionic species is treated as a neutral species by the addition of a proton. When there was more than one way to attach a proton to a charged complex, we explored all possibilities and chose the most stable species. In the case of $[V(O)_2(pca)_2]$, the most stable neutral complex is the one in which the proton is added to a vanadyl group.

i. $V(O)_2(pca)(CH_3CN) + pcaH + OH^- = [V(O)_2(pca)_2]^- + CH_3CN + H_2O$

ii. $V(O)_2(pca)(CH_3CN) + pcaH = V(O)(OH)(pca)_2 + CH_3CN$

Unrestricted density functional theory (DFT) calculations were performed using the B3LYP functional,[4] and the 6-31G* basis set was used for all atoms. All electronic structure calculations were done using the *Q-Chem 2.02* program package.[5] Transition states for all reactions were determined using the growing string method.[6] Intrinsic reaction coordinate (IRC) calculations were performed for all transition state structures to confirm that these structures are properly related to the expected reactant and product states.

Equilibrium constants and rate constants were calculated using statistical mechanics and absolute rate theory.[7] Since we do not have a reliable way to approximate the translation and rotational partition functions in solution, equilibrium constants were calculated on the basis of only the electronic degrees of freedom, and the contributions of translational, rotational, and vibrational degrees of freedom were neglected. In the discussion of our results, we show that the inclusion of all degrees of freedom in the calculations of rate constants, as would be done for gas-phase reactions, results in an overestimation of the entropic effects for reactions occurring in the liquid phase.

Results and Discussion

Vanadium/PCA System. Shul'pin et al. have reported that the reaction of *n*-Bu_4NVO_3 with PCA results in an equilibrium mixture of vanadium−pca complexes containing one and two pca ligands.[3] ^1H and ^{51}V NMR spectra showed that treatment of *n*-$Bu_4N(VO_3)$ with PCA in acetonitrile-d_3 results in the formation of a new product. Reaction was complete at about 2 equiv of PCA, and higher concentrations of PCA did not lead to any additional species. On the basis of this observation, it was concluded that the vanadium complex with two pca ligands is the only species present in an equilibrated solution when $[PCA]_0/[V]_0 > 2$. In support of this conclusion, the authors reported that *n*-$Bu_4N^+[VO_2(pca)_2]^-$ was crystallized from an acetonitrile solution.[8]

We have represented the reaction of VO_3^- anions with pca by reactions 1 and 2 in Table 1. As noted earlier, VO_3^- is replaced by $HOVO_2$, to avoid dealing with anionic species. Values of ΔE and equilibrium constants for these reactions are also given in Table 1. Figure 2 illustrates the distribution of vanadium complexes involving one and two pca ligands as a function of the concentration of PCA. Our model predicts that the concentration of species **2** increases as the concentration of PCA increases from 0 to approximately 1 equiv of vanadium, at which point all vanadium is in the form of complex **2**. Upon further increase in PCA concentration, a complex with two pca ligands (**3**) is formed. However, a significant concentration of **2** (20% of all vanadium species) remains even when $[PCA]_0/[V]_0 \approx 10$. Although reaction 2 is exothermic by −29 kJ/mol, not all of the vanadium is predicted to be in complex **3**, because reaction 2 represents a competition between PCA ligands and acetonitrile molecules for sites in the vanadium coordination

TABLE 1: Model Reactions Used in This Work

	reaction	ΔE, kJ/mol		K at 40 °C	
		a[a]	d[b]	a[a]	d[b]
1	$HOVO_2(CH_3CN)_2$ (**1**) + pcaH ↔ VO_2(pca)(CH_3CN) (**2**) + H_2O + CH_3CN	−39	3.0×10^6 mol/L		
2	VO_2(pca)(CH_3CN) + pcaH ↔ (HO)VO(pca)$_2$ (**3**) + CH_3CN	−29	8.1×10^4		
3	VO_2(pca)(CH_3CN) + H_2O_2 ↔ VO_2(pca)(H_2O_2) (**4**) + CH_3CN	−14	−15	2.0×10^2	5.0×10^2
4	VO_2(pca)(H_2O_2) + H_2O + CH_3CN ↔ $HOVO_2(CH_3CN)(H_2O_2)$ (**5**) + pcaH	10	13	1.8×10^{-2} L/mol	7.2×10^{-3} L/mol
5	(HO)VO(pca)$_2$ + H_2O_2 ↔ (HO)VO(pca)$_2$(H_2O_2) (**6**)	N/A	0 L/mol		
6	VO_2(pca)(H_2O_2) → VO(OH)(pca)(OOH) (**7**)	see Table 2			
7	VO(OH)(pca)(OOH) + CH_3CN → •VO(OH)(pca)(CH_3CN) (**8**) + HOO•	see Table 2			

[a] Robot's arm pathway. [b] Direct pathway.

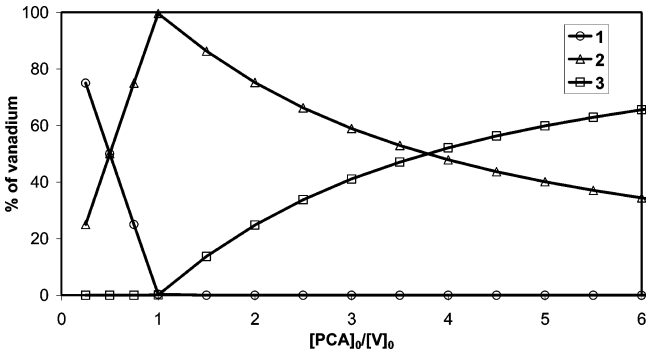

Figure 2. Calculated vanadium distribution in vanadate/PCA mixtures (complexes **1**−**3**).

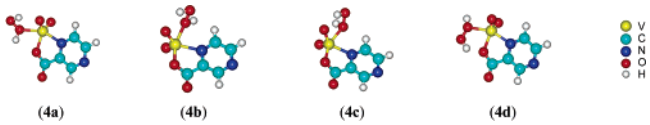

Figure 3. H_2O_2 adsorption complexes with **2**.

sphere. Since the concentration of solvent is much higher than the concentration of PCA, the equilibrium distribution is shifted toward **2**. While the results presented in Figure 2a are qualitatively consistent with the observations of Shul'pin et al.,[3] the crossing of the curves for **2** and **3** determined theoretically occurs at a much higher value of $[PCA]_0/[V]_0$ than that observed experimentally, $[PCA]_0/[V]_0 = 1$. We believe that this discrepancy is only apparent, since the ^{1}H NMR signals of complexes **2** and **3** are expected to be very similar and hence indistinguishable. Consequently, it is likely that what Shul'pin et al.[3] report as the concentration is the sum of the concentrations of **2** and **3**, and not the concentration of **3** alone. We also note that the observation of crystalline **3** upon solvent evaporation is consistent with our theoretical predictions, since solvent evaporation would shift the equilibrium of reaction 2 toward **3**.

H_2O_2 Coordination. According to Shul'pin et al.,[3] H_2O_2 coordinates to vanadium complexes containing different numbers of pca ligands. The resulting species are shown in Table 1 as complexes **4**, **5**, and **6**. Complex **5** does not contain a pca ligand, whereas complexes **4** and **6** contain one and two pca ligands, respectively.

To find stable configurations for **4**, we considered several possible ways to attach H_2O_2 to complex **2**. The minimum-energy structures are shown in Figure 3. In complexes **4a** and **4d**, H_2O_2 is located opposite the N atom of the pca ligand, while in complexes **4b** and **4c**, H_2O_2 is coordinated opposite the O atom of the pca ligand. Calculation of the relative stability of these four structures predicts that an equilibrium mixture at 40 °C consists of 39% of **4a** and 61% of **4d**. The fraction of **4c** is less than 0.02%, and the fraction of **4b** is negligible. Thus, only **4a** and **4d** are considered for further discussion. While complexes **4a** and **4d** differ in the way that the hydrogen atoms of the hydroperoxide are oriented with respect to the other ligands, it is expected that in solution rapid equilibration between these species occurs via rotation of H_2O_2 around the V−O bond. As discussed below, complexes **4a** and **4d** represent precursors to the robot's arm and direct mechanisms, respectively. In complex **4a**, the migrating H atom is close to the oxygen atom of the pca ligand, whereas in complex **4d**, the H atom is close to a vanadyl group.

We also considered the coordination of H_2O_2 with VO_2(OH)-(pca)$_2$ (complex **3**). The vanadium atom in **3** has a coordination number of 6 (actually 5, if one recognizes that the dative V−N bond is significantly longer than the other bonds to V). Since the usual coordination number of V in this type of complex is 5, H_2O_2 is not expected to fit into the coordination shell. Our calculations confirm this conclusion. All attempts to find minima for structures such as **6** led to complexes with unbound H_2O_2. That is why H_2O_2 can only replace one pca ligand in the coordination sphere leading to the formation of the coordination complexes discussed earlier (**4a**, **4d**). The calculated instability of the complex between H_2O_2 and **3** is consistent with the proposal of Shul'pin et al.[3] that complex **1** is the only precursor to the catalytically active species responsible for the free radical generation.

The energies and equilibrium constants for H_2O_2 adsorption are given in Table 1 (reactions 3, 4, and 5). The calculated equilibrium constants were used to determine the distribution of vanadium complexes as functions of the initial concentrations of PCA and H_2O_2. Details concerning these calculations are given in the Appendix. Figure 4A shows that, as the PCA concentration is increased, while keeping the concentration of H_2O_2 at 2000 equiv of vanadium, the dominant complex, **5**, which contains only H_2O_2 and solvent ligands, is replaced by complex **3**, which contains two pca ligands. At a constant PCA concentration of 4 vanadium equiv, increasing the H_2O_2 concentration leads to the replacement of complexes **2** and **3** by **5** (Figure 4B).

Figure 5A shows the calculated concentrations of **4d** and **4a** as a function of the ratio of the initial concentration of PCA to the initial concentration of vanadium, $[PCA]_0/[V]_0$ (the initial concentration of H_2O_2 is held constant at $[H_2O_2]_0/[V]_0 = 2000$). The concentration of **4d** increases with increasing $[PCA]_0/[V]_0$ and then passes through a maximum corresponding to 5% of $[V]_0$ for $[PCA]_0/[V]_0 = 130$. The same pattern is predicted for **4a**, which reaches a maximum of 2% of $[V]_0$ at $[PCA]_0/[V]_0 = 130$. A comparison of the results shown in Figure 5 with the experiments of Shul'pin et al.[3] cannot be done directly, since the concentration of **4** was not measured in the experimental studies. However, since Shul'pin et al. assumed that the rate of alkane oxidation is directly proportional to the concentration of **4**, an apparent concentration of **4** can be determined by dividing the observed rate of alkane oxidation by the rate coefficient for the rate-limiting step. With this approach, the concentration of **4** versus $[PCA]_0/[V]_0$ was determined from the

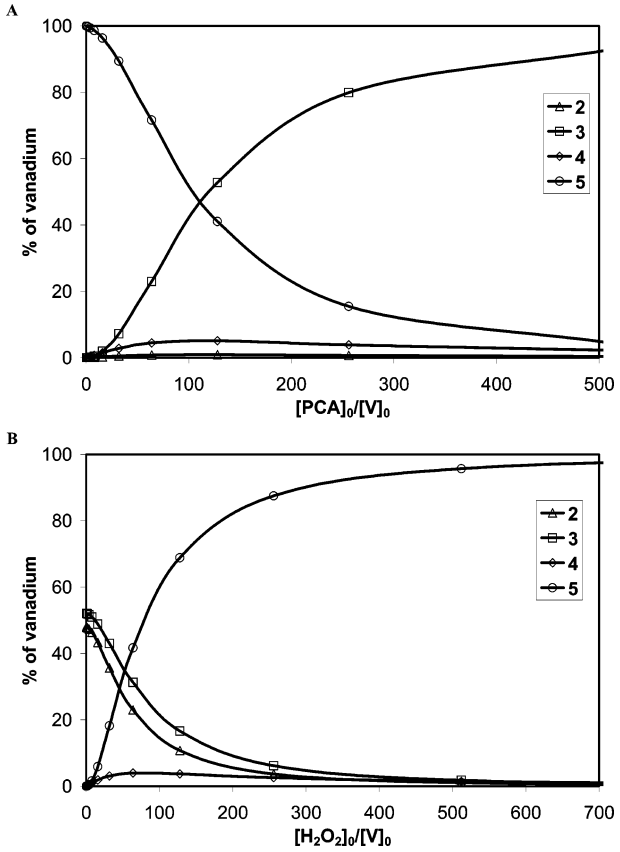

Figure 4. Calculated vanadium distribution in the mixture of vanadate/PCA/H_2O_2: (A) as a function of initial PCA concentration $[PCA]_0$, $[H_2O_2]_0 = 2000 \times [V]_0$, (B) as a function of initial H_2O_2 concentration $[H_2O_2]_0$, $[PCA]_0 = 4 \times [V]_0$. Direct pathway distribution is shown; indirect pathway gives almost identical curves and is not shown on this plot. Complex **1** is not shown because its concentration is negligible.

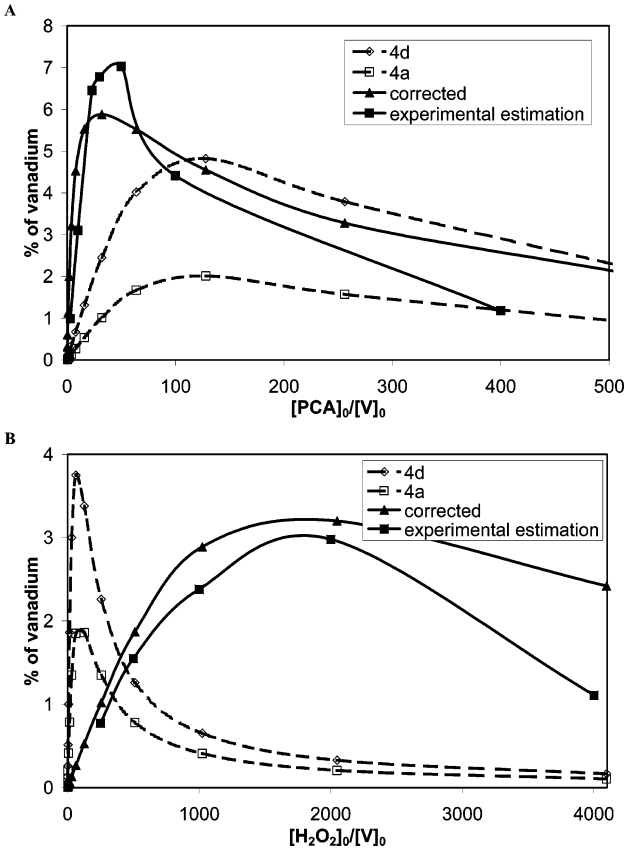

Figure 5. Concentrations of species **4** in the mixture of vanadate/PCA/H_2O_2 estimated from experiment and calculated from theory. Corrected values are shown for $K_2 = 1.1 \times 10^3$, $K_3 = 7.9$, $K_4 = 4.5 \times 10^{-4}$ L/mol: (A) as a function of initial PCA concentration $[PCA]_0$, $[H_2O_2]_0 = 2000 \times [V]_0$, (B) as a function of initial H_2O_2 concentration $[H_2O_2]_0$, $[PCA]_0 = 4 \times [V]_0$.

data of Shul'pin et al.[3] for hexane oxidation, taking the rate coefficient for the rate-limiting step to be 0.4 s^{-1}. The resulting curve is shown in Figure 5A. While the experimental and theoretical curves are similar in shape, the curve based on experimental data reaches a maximum of 7% of $[V]_0$ at $[PCA]_0/[V]_0 = 50$.

The effect of H_2O_2 concentration on the concentrations of **4d** and **4a** is shown in Figure 5B for a fixed value of $[PCA]_0/[V]_0 = 4$. Also shown is a curve for **4** calculated from the work of Shul'pin et al.[3] in same manner as that discussed above. As the concentration of H_2O_2 increases, the concentration of **4** passes through a maximum in accordance with the experimentally observed behavior. Although the calculated value of the peak (2−4% of $[V]_0$) agrees with that observed experimentally (3% of $[V]_0$), the position of the predicted maximum does not coincide well with that seen in the experimental results (theoretical 100 equiv H_2O_2 vs experimental 2000 equiv).

The discrepancies between the calculated and experimental curves shown in Figure 5A,B are attributable to the exclusion of entropy changes associated with reactions 1−4 as part of the calculations of K_1−K_4. As noted in the section on Theoretical Approach, accurate determination of the entropy change for liquid-phase reactions is much more difficult than for gas-phase reactions because of the need to capture the influence of solute−solvent interactions in the calculations. It is possible, however, to set upper limits on the corrections to K_1−K_4 based on estimates of the entropy changes which would occur if each of these reactions were carried out in the gas phase. For reactions 2 and 3, which do not involve a change in the number of moles, the values of K_2 and K_3 are estimated to change by no more than 2 orders of magnitude upon inclusion of the entropy of reaction, whereas the values of K_1 and K_4 could change by as much as 5 orders of magnitude, since both reactions involve changes in the number of moles. Working with these constraints, we examined the effects of changes in K_2−K_4 on the distribution of **4** with changes in $[PCA]_0/[V]_0$ and $[H_2O_2]_0/[V]_0$. The value of K_1 was not adjusted upward to account for the positive change in the entropy of reactions, since reaction 1 will be complete even for $K_1 = 3.0 \times 10^6$. The final values of the constants are $K_1 = 3.0 \times 10^6$ mol/L, $K_2 = 1.1 \times 10^3$, $K_3 = 7.9$, and $K_4 = 4.5 \times 10^{-4}$ L/mol. Figure 5A,B shows that the new values K_2, K_3, and K_4 result in significantly better agreement of the calculated curves with the experimental estimation.

If the adjusted value of K_2 is used to determine the distribution of **1**, **2**, and **3** in a vanadium/PCA mixture, then essentially the same results are obtained with the concentration of **2** dropping more slowly than shown in Figure 2.

Free Radical Generation via the Decomposition of VO_2(pca)(H_2O_2). Shul'pin et al.[3] have proposed that VO_2(pca)(H_2O_2) (**4**) generates hydroperoxyl radicals, $HOO^\bullet$, via a two-step process (see Figure 1). In the first step, an H atom migrates from the adsorbed H_2O_2 to the O atom of a vanadyl group, and in the second step, an $HOO^\bullet$ radical is released from the newly formed complex. Both of these steps were examined theoretically in the course of the present investigation (reactions 6 and 7 in Table 1).

As mentioned earlier, two pathways were considered for hydrogen transfer to a vanadyl group. In the direct pathway,

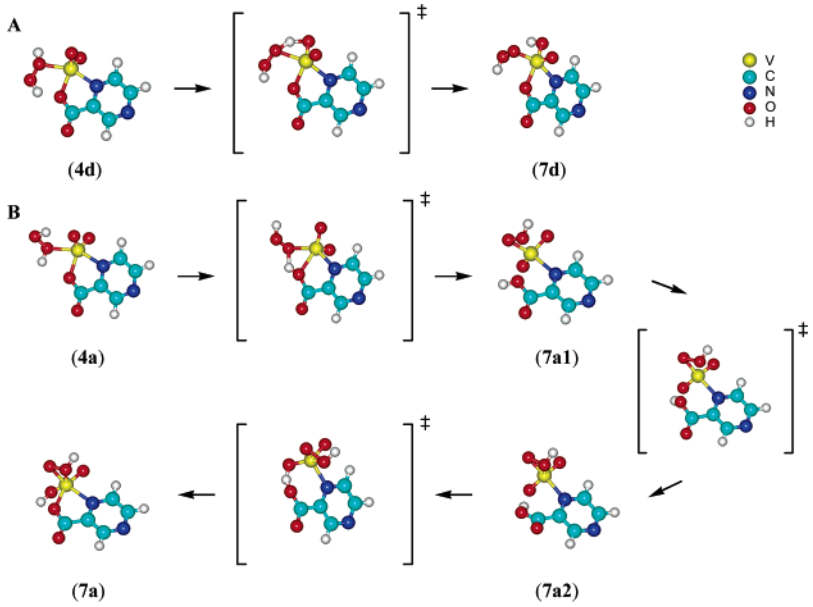

Figure 6. Hydrogen migration via direct (A) and "robot's arm" (B) mechanisms.

TABLE 2: Calculated Activation Energies and Rate Constants (40 °C) for Hydrogen Transfer and HOO• Generation

reaction	E^{act}, kJ/mol	ΔE^{act}_{rev}, kJ/mol	k, s^{-1}	k_{rev}, s^{-1}
6d: **4d** to **7d**	99	137	1.7×10^{-4}	8.6×10^{-11}
6a1: **4a** to **7a1**	81	52	1.9×10^{-1}	1.6×10^{4}
6a2: **7a1** to **7a2**	30	22	5.5×10^{7}	1.7×10^{9}
6a3: **7a2** to **7a**	29	70	8.4×10^{7}	1.5×10^{1}

	S_N1	S_N2	S_N1	S_N2	S_N1	S_N2	S_N1	S_N2
7d: **7d** to **8**	192	>141	51	>0	6.0×10^{-20}	2.0×10^{-11}	1.9×10^{4}	N/A
7a: **7a** to **8**	154	>103	51	>0	1.3×10^{-13}	4.5×10^{-5}	1.9×10^{4}	N/A

TABLE 3: HOO• Generation: S_N1-Type and S_N2-Type Reactions

type	reactions
S_N1	VO(OH)(pca)(OOH) (**7a** or **7d**) → •VO(OH)(pca) (**9**) + HOO•
	•VO(OH)(pca) + CH_3CN → •VO(OH)(pca)(CH_3CN) (**8**)
S_N2	VO(OH)(pca)(OOH) (**7a** or **7d**) + CH_3CN→ [VO(OH)(pca)(OOH)(CH_3CN)]‡
	[VO(OH)(pca)(OOH)(CH_3CN)]‡ → •VO(OH)(pca)(CH_3CN) (**8**) + HOO•

hydrogen transfer occurs in one step as shown in Figure 6A (see also Table 2, reaction 6d), whereas the indirect pathway involves a series of intermediate states. The hydrogen atom first migrates to the oxygen atom of the pca ligand connected to the vanadium atom as shown in Figure 6B (reaction 6a1 in Table 2). The pca ligand brings the hydrogen atom closer to a vanadyl group (see Figure 6B and reaction 6a2 in Table 2), and the hydrogen atom then transfers to the vanadyl group (see Figure 6B and Reaction 6a3 in Table 2). Contrary to the suggestion of Shul'pin et al.,[3] we find that an H atom of H_2O_2 cannot be transferred to the nitrogen atom involved in the dative bond to vanadium, since this process would involve either breaking of a strong V−N bond or destabilization of the aromatic system in the pca ligand. The activation energies for the forward and reverse processes, as well as rate coefficients for each step, are given in Table 2.

The key step in the oxidation of hydrocarbons by the vanadate/PCA/H_2O_2 system is proposed to be the generation of free radicals. To describe the kinetics of this process, we have determined the internal energy changes and the activation barriers associated with the elementary steps leading to the release of HOO• radicals. In our model, a solvent molecule replaces HOO• from complexes **7d** and **7a** with the formation of complex **8** (Table 3). This substitution can occur via an S_N1 or S_N2 mechanism. The intermediate for the S_N1 process (**9**) is just complex **7** with a broken V−OOH bond. The energetics of the step are summarized in Table 2 (reactions 7d and 7a).

To explain the observed rate of cyclohexane oxidation (~10^{-6} mol/(L × s)), rate constants for the key step should be on the order of unity, since the calculated concentration of the precursors is 10^{-6} mol/L. One can see from Table 2 that the rate coefficients for S_N1 substitution of HOO• by CH_3CN are too small to be consistent with the observed rates.

The S_N2 reaction is expected to have a lower-energy transition state, since both the OOH group and CH_3CN are bonded to vanadium. These interactions lower the overall energy of the system. Unfortunately, despite extensive effort, a transition state for reaction 7 could not be determined. Since the reaction of interest is endothermic, a lower bound on the activation energy is given by the internal energy change, which is positive. This lower bound is 141 kJ/mol for reaction 7d and 103 kJ/mol for reaction 7a. Since the preexponential factor is taken to be (kT/h), the lower bound on the rate coefficient at 40 °C is 2.0×10^{-11} s^{-1} and 4.5×10^{-5} s^{-1} for the direct and indirect mechanisms, respectively. The activation energy for the S_N1 reaction gives the upper bound on the activation energy.

As noted earlier, Shul'pin et al.[3] assume the rate at which HOO• radicals are formed to be equivalent to the overall rate of alkane oxidation, since the former process is rate-limiting. As described in the Appendix, we calculated the rate of alkane

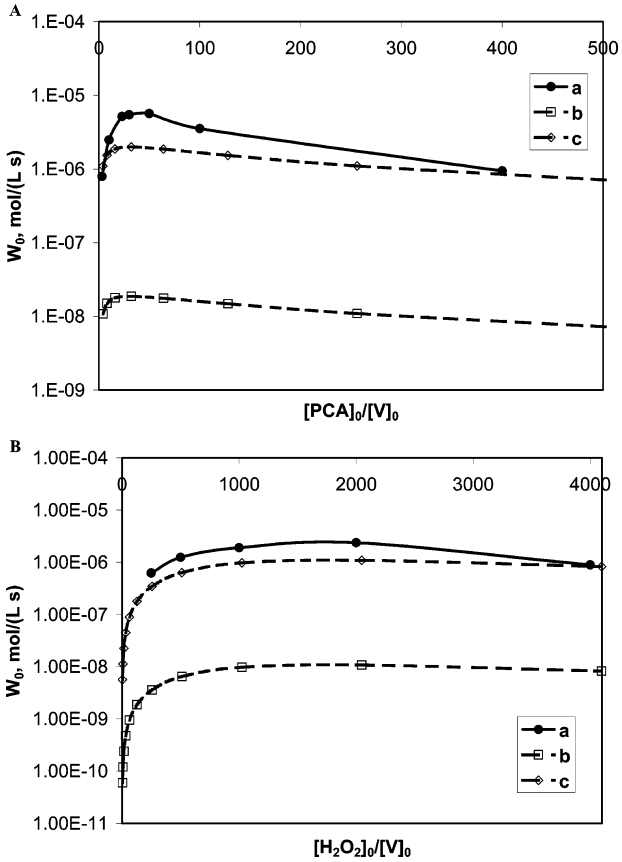

Figure 7. Theoretical (S_N2 mechanism) and experimental rates: (A) as a function of initial PCA concentration $[PCA]_0$, $[H_2O_2]_0 = 2000 \times [V]_0$, (B) as a function of initial H_2O_2 concentration $[H_2O_2]_0$, $[PCA]_0 = 4 \times [V]_0$. Curve a, experimental rate; curve b, calculated with reaction 7a as the rate-determining step; curve c, calculated with reaction 6a1 as the rate-determining step.

(cylcohexane) oxidation as a function of the initial concentrations of PCA and H_2O_2. The results are presented in Figure 7 (curve b) together with the experimentally reported rate (curve a). Although the theoretically determined oxidation rate exhibits a maximum consistent with what is observed experimentally, the calculated rates are 3 orders of magnitude lower than the experimental ones. The reason for the discrepancy is the high activation barrier for the dissociation of the V−OOH bond (reaction 7a). The activation energy of this step was estimated on the basis of B3LYP energies of the minimum-energy structure, for which B3LYP is accurate. Therefore, the major source of error in the calculations might be the failure to take into account entropy effects when calculating rate coefficients for reactions 6 and 7. Taking into account the activation entropy will increase the rate of the hydrogen transfer step via the S_N1 mechanism by at most 5 orders of magnitude. As can be seen from Table 2, this is still not enough to describe the observed rates. The activation entropy will significantly slow the rate via the S_N2 process (the transition state is more ordered than the reactants). Therefore, correcting for the entropy of activation will result in a prediction of even lower oxidation rates. These observations lead us to conclude that alternative pathways for the generation of free radicals need to be considered.

Alternative Pathways for Radical Generation. We considered a number of alternatives to reaction 7 as possible pathways for the formation of free radicals. As shown in Table 4, all of the alternative paths involve the generation of HO$^\bullet$ or HOO$^\bullet$ radicals with or without solvent participation, as well as with O_2 participation. The estimated lower bounds on ΔE_{act} are given in Table 4. None of the proposed processes has an activation barrier for free radical generation that is lower than that for reaction 7, 103 kJ/mol. Therefore, we can conclude that even if the free radicals are formed from **7a** this process is slower than the observed rate of alkane oxidation.

Another possibility is that free radicals are not formed directly from **7a** but are formed instead via a sequence of steps starting from this complex. A plausible pathway for such a sequence is given in Figure 8. A solvent molecule first displaces water from **7a**. This, of course, is not an elementary step and includes at least one hydrogen transfer. However, we have already shown that the hydrogen transfer that occurs via the indirect mechanism has a reasonably low activation barrier (80−90 kJ/mol). The total energy of the system decreases in reaction 8. Furthermore, experimental observation confirms that complexes containing O_2 ligand(s) (e.g., **10**, **15**) are the components in vanadium/H_2O_2 systems.[9] The formal coordination number of vanadium is 6 in complex **10**; however, since O_2 does not form two σ bonds with the vanadium atom, it is considered to be a monodentate ligand, resulting in a coordination number 5. In the next step (reaction 9), H_2O_2 replaces a solvent molecule coordinated to **10**, resulting in the formation of an analogue of **4** with one vanadyl group replaced by O_2 (**11**). This complex can also undergo indirect hydrogen migration to form **12**, which in turn can eliminate an HOO$^\bullet$ radical via an S_N2 (reaction 11) or S_N1 (reaction 12) process. We observe that complex **12** can also eliminate water (reaction 13), starting a new cycle of H_2O_2 coordination (reaction 14), hydrogen migration (reaction 15), and HOO$^\bullet$ elimination (reactions 16 and 17). By analogy with reaction 7, we can estimate the lower and upper bounds on the activation barrier as ΔE for the S_N2 and S_N1 processes. As we see from Figure 8, the range of activation barriers is 88−150 kJ/mol for the elimination of HOO$^\bullet$ from **12** and 85−124 kJ/mol for the elimination from **17** versus 103−154 kJ/mol starting from **7a**. We have summarized the estimated barriers for HOO$^\bullet$ formation from **7a**, **12**, and **17** in Table 5. The energetic profile of the overall process is shown in the Figure 9. In this figure, we only show transition states for reactions 6a1, 6a2, and 6a3. All other transition states between complexes **7a** and **12**, and between **12** and **17**, will not affect the overall kinetics. The most important observation from Figure 9 is that the activation barriers for free radical formation from **12** and **17** are lower than that from **7a**. Therefore, we can consider reactions 11 and 16 as plausible pathways for the generation of HOO$^\bullet$ radicals. Another important observation is that the barrier for HOO$^\bullet$ generation from **17** is comparable to the barrier for indirect hydrogen transfer (reaction 6a1). Therefore, the hydrogen transfer step can also become the rate-limiting step in the overall process. This observation is in agreement with the hypothesis of Shul'pin et al. that the catalytic activity of the catalyst is determined by the ability to transfer proton from hydrogen peroxide to a vanadyl group.

We determined the rate of HOO$^\bullet$ formation, assuming that hydrogen migration via reaction 6a1 is the rate-determining step and that all processes after this reaction occur rapidly. Figure 7 shows the rate of HOO$^\bullet$ formation as a function of the initial concentrations of PCA and H_2O_2 (curve c). Also shown in this plot are the experimental data (curve a) and the rate calculated for the previous model (reaction 7a as the rate-determining step, curve b). It is evident that the new model gives results that are within 1 order of magnitude of the experimental data and 2 orders of magnitude better than the previous model. However, one should be aware of the errors in B3LYP energies for the transition states. Even though agreement within an order of

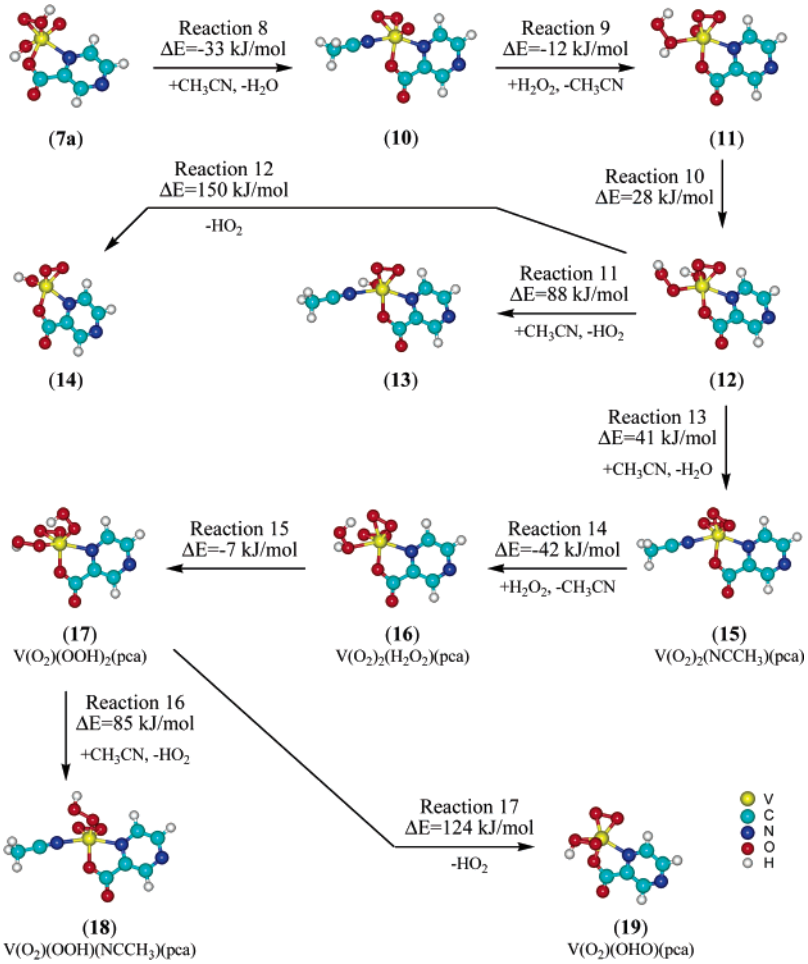

Figure 8. Alternative pathway for HOO• generation. Line formulas are given wherever vanadium ligands are not clearly visible.

TABLE 4: Alternative Pathways for (O)V(OOH)(OH)(pca) (7a) Decomposition

reaction	lower bound on ΔE_{act}, kJ/mol
(O)V(OOH)(OH)(pca) →HardReturn•V(O)$_2$(OH)(pca) + HO•	173
(O)V(OOH)(OH)(pca) →HardReturn•V(O)(OOH)(pca) + HO•	270
CH_3CN + (O)V(OOH)(OH)(pca) →HardReturn•V(O)$_2$(OH)(CH_3CN)(pca) + HO•	163
CH_3CN + (O)V(OOH)(OH)(pca) →HardReturn•V(O)(OOH)(pca)(CH_3CN) + HO•	217
O_2 + (O)V(OOH)(OH)(pca) →HardReturn•V(O)(O_2)(OH)(pca) + HOO•	113
O_2 + (O)V(OOH)(OH)(pca) →HardReturn•V(O)(O_2)(OOH)(pca) + HO•	168

TABLE 5: Kinetic Parameters for HOO• Formation

initial complex	**7a**	**12**	**17**
ΔE_{act} range, kJ/mol	103−154	88−150	85−124
k range, s^{-1}	4.5×10^{-5}−1.3×10^{-13}	1.3×10^{-2}−6.6×10^{-13}	3.9×10^{-2}−1.3×10^{-8}
apparent ΔE_{act} range, kJ/mol	85−136	67−115	67−81
experimental apparent activation energy, kJ/mol		63−80	

magnitude for the reaction rates is usually considered very good, more accurate theoretical prediction of the reaction rates requires employment of more reliable methods for determination of transition state energies.

The experimentally measured activation energy 63−80 kJ/mol agrees very well with the theoretical value for the apparent activation energy. The apparent activation energy is calculated as the difference between the energy of the highest transition state along the reaction pathway (Figure 9) and the energy of the starting compounds. The lower bound of the apparent activation energy is determined by the height of the peak (with respect to the energy of the starting point) of either the hydrogen transfer step or HOO• elimination step, whichever is higher. On the basis of the agreement of the apparent activation energy for HOO• formation from **17** (67−81 kJ/mol) with that observed experimentally, we can conclude that HOO• generation originating from this complex is reasonable.

Conclusions

DFT calculations of reaction energetics were used to verify the plausibility of the mechanism of hydrocarbon oxidation by a vanadate/PCA/H_2O_2 catalyst proposed by Shul'pin et al.[3] on the basis of experimental observations. Despite its simplicity, the proposed model is capable of reproducing the major trends seen experimentally. Predicted dependences of the oxidation rate

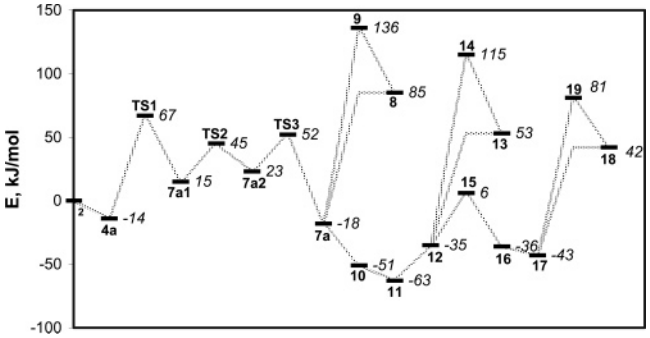

Figure 9. Energy profile for the proposed mechanism. Numbers in italic represent the energy of the state. TS1, TS2, and TS3 correspond to the transition states between **4a** and **7a1**, **7a1** and **7a2**, and **7a2** and **7a**, respectively (see Figure 6).

on initial concentrations of PCA and H_2O_2 have characteristic maxima. This shape is determined by the equilibrium concentration of the active species. As correctly deduced by Shul'pin et al.,[3] vanadium complexes with one pca and one H_2O_2 ligand are the major catalytically active species. H_2O_2 adsorption complexes without pca are less active, since they can be converted only through the direct hydrogen transfer. Our calculations show that direct hydrogen transfer from the H_2O_2 molecule to a vanadyl group has a higher barrier and, therefore, a much lower rate. Indirect transfer occurs by migration of hydrogen from coordinated H_2O_2 to the oxygen of a pca ligand connected to the vanadium atom. In contradiction to what was proposed by Shul'pin et al.[3] we find that the nitrogen atom of the pca ligand cannot participate in hydrogen transfer and that species containing two pca ligands and an H_2O_2 molecule do not exist in the solution. The maximum in the rate of oxidation as a function of $[PCA]_0$ is attributable to the predominance of vanadium complexes with two pca ligands at high initial PCA concentration. The maximum in the rate of oxidation versus $[H_2O_2]_0$ is attributable to the retarding effect of water, which is part of the hydrogen peroxide solution. Our work has shown that the generation of $HOO^\bullet$ radicals cannot occur via direct cleavage of a V−OOH bond, since the activation barrier for this process is too high. Instead, $HOO^\bullet$ radicals are formed via a sequence of steps involving lower activation barriers. For our mechanism, the rate of V−OOH bond breakage is lower than the rate of the hydrogen transfer from coordinated hydrogen peroxide molecule to a vanadyl group. Thus, the latter becomes the rate-determining step. The new mechanism for free radical generation underestimates the observed rate of hexane oxidation by less than an order of magnitude. Part of this error may be attributed to the failure of DFT to calculate accurate energies of the transition states. The entropy change in the hydrogen transfer is expected to be small and will not affect the barrier significantly. However, the tunneling effects for such a light atom as hydrogen may be responsible for the underestimation. The activation energy measured experimentally (63−80 kJ/mol) agrees very well with calculated values (67−81 kJ/mol). The proposed mechanism also explains the important role of the cocatalyst in the reaction, which acts as a robot's arm in the transfer of hydrogen. The energy profile of the overall process (Figure 9) suggests that it might not be possible to find a better cocatalyst than PCA. The reason is that there are two energetic barriers of approximately the same height on the proposed pathway (see Figure 9) corresponding to the transfer of hydrogen and V−OOH bond breakage. While changing the cocatalyst might lower the activation barrier for the transfer of hydrogen (**TS1**), it will have only a slight effect on the second barrier, leaving the overall rate unchanged. Finally, the calculations reported here show that coordination of the solvent, acetonitrile, to vanadium complexes becomes important and plays significant role in the reactions.

Appendix

Equilibrium Distribution of Vanadium-Containing Species in Vanadate/PCA/H_2O_2 Mixtures. The distribution of vanadium-containing species in vanadate/PCA/H_2O_2 mixtures was determined analytically by solving the equation describing equilibrium for reactions 1−4 and an overall mole balance on vanadium and PCA. The equilibrium concentrations of H_2O_2, water, and acetonitrile were taken to be identical to their initial concentrations, since the concentrations of these components are much higher than those of all vanadium-containing species and hence do not change significantly during equilibration. The same assumption cannot be used for the concentration of PCA, since it leads to a solution that does not predict a maximum in the dependence of the concentration of **4** on the initial concentration of H_2O_2. The following standard concentrations were used for all calculations unless otherwise stated: $[\mathbf{1}]_0 = 1.0 \times 10^{-4}$ mol/L, $[PCA]_0 = 4.0 \times 10^{-4}$ mol/L, $[H_2O_2]_0 = 2.0 \times 10^{-1}$ mol/L, $[H_2O]_0 \approx 0.757$ mol/L (33.33% H_2O_2 aqueous solution), $[CH_3CN]_0 = 18.536$ mol/L.

Kinetics. The changes in the concentrations of all vanadium species with time were determined analytically by solving the set of differential kinetic equations describing the rates of formation and consumption of species **4**, **7a1**, **7a2**, and **7**. The initial concentrations for all species except **4** were taken to be zero. The initial concentration of **4** is given by the equilibrium concentration in the equilibrated mixture. During the calculation, the concentration of this species was allowed to re-equilibrate after each second of system evolution. We also assumed that the final species **8** is immediately converted back to **2**, which means that the final consequence of the reaction is the conversion of H_2O_2 into $HOO^\bullet$ and $H^\bullet$. $H^\bullet$ is implicitly formed when **8** is converted to **2**. The standard concentrations noted above were used for all species unless otherwise stated. For these conditions, the concentrations of intermediate species are very small at all times and never exceed 10^{-6} of the initial vanadium concentration. After initiation, the rate of $HOO^\bullet$ formation is essentially constant, meaning that the concentration of $HOO^\bullet$ increases linearly with time. In accordance with the scheme in Figure 1, every $HOO^\bullet$ generated in the system produces an additional $HO^\bullet$ radical. Therefore, the rate of oxidation is twice the rate of $HOO^\bullet$ formation.

Acknowledgment. This work was supported by the Director, Office of Basic Energy Sciences, Chemical Sciences Division of the U.S. Department of Energy under contract DE-AC03-76SF00098.

References and Notes

(1) (a) Sheldon, R. A.; Kochi, J. K. *Metal-Catalyzed Oxidations of Organic Compounds*; Academic Press: New York, 1981. (b) *Catalytic Oxidation with H_2O_2 as Oxidant*; Strukul, G., Ed.; Kluwer Academic Publishers: Dordrecht, 1992. (c) Shilov, A. E.; Shul'pin, G. B. *Activation and catalytic reactions of saturated hydrocarbons in the presence of metal complexes*; Kluwer Academic Publishers: Boston, 2000. (d) Shilov, A. E.; Shul'pin, G. B. *Chem. Rev.* **1997**, *97*, 2879.

(2) (a) Shul'pin, G. B.; Attansio, D.; Suber, L. *Russ. Chem. Bull*. **1993**, *42*, 55. (b) Shul'pin, G. B.; Druzhinina, A. N.; Nizova, G. V. *Russ. Chem. Bull*.**1993**, *42*, 1327. (c) Nizova, A. N.; Shul'pin, G. B. *Russ. Chem. Bull*. **1994**, *43*, 1146. (d) Shul'pin, G. B.; Süss-Fink, G. *J. Chem. Soc., Perkin Trans. 2* **1995**, 1459. (e) Shul'pin G. B.; Drago, R. S.; Gonzalez, M. *Russ. Chem. Bull.* **1996**, *45*, 2386. (f) Guerreiro, M. C.; Schuchardt, U.; Shul'pin, G. B. *Russ. Chem. Bull.* **1997**, *46*, 749. (g) Shul'pin, G. B.; Guerreiro, M. C.; Schuchardt, U. *Tetrahedron* **1996**, *52*, 13051. (h) Nizova, G. V.; Süss-

Fink, G.; Shul'pin, G. B. *Tetrahedron* **1997**, *53*, 3603. (i) Schuchardt, U.; Guerreiro, M. C.; Shul'pin, G. B. *Russ. Chem. Bull*. **1998**, *47*, 247. (j) Süss-Fink, G.; Nizova, G. V.; Stanislas, S.; Shul'pin, G. B. *J. Mol. Catal. A: Chem*. **1998**, *130*, 163. (k) Shul'pin, G. B.; Ishii, Y.; Sakaguchi, S.; Iwahama, T. *Russ. Chem. Bull.* **1999**, *48*, 887.

(3) Shul'pin, G. B.; Kozlov, Y. N.; Nizova, G. V.; Süss-Fink, G.; Stanislas, S.; Kitaygorodskiy, A.; Kulikova, V. S. *J. Chem. Soc., Perkin Trans. 2* **2001**, 1351.

(4) (a) Parr, R. G.; Yang, W. *Density-Functional Theory of Atoms and Molecules*; Oxford University Press: Oxford, U.K., 1989. (b) Becke, A. D. *J. Chem. Phys.* **1993**, *98*, 5648. (c) Lee, C.; Yang, W.; Parr, R. G. *Phys. Rev. B* **1988**, *37*, 785.

(5) Kong, J.; White, C. A.; Krylov, A. I.; Sherrill, C. D.; Adamson, R. D.; Furlani, T. R.; Lee, M. S.; Lee, A. M.; Gwaltney, S. R.; Adams, T. R.; Ochsenfeld, C.; Gilbert, A. T. B.; Kedziora, G. S.; Rassolov, V. A.; Maurice, D. R.; Nair, N.; Shao, Y.; Besley, N. A.; Maslen, P. E.; Dombroski, J. P.; Dachsel, H.; Zhang, W. M.; Korambath, P. P.; Baker, J.; Byrd, E. F. C.; Van Voorhis, T.; Oumi, M.; Hirata, S.; Hsu, C. P.; Ishikawa, N.; Florian, J.; Warshel, A.; Johnson, B. G.; Gill, P. M. W.; Head-Gordon, M.; Pople, J. A. *Q-Chem*, version 2.02; Q.-Chem, Inc., Export, PA, 2000.

(6) Peters, B.; Heyden, A.; Bell, A. T.; Chakraborty, A. *J. Chem. Phys.* **2004**, *120*, 7877.

(7) (a) McQuarrie, D. A. *Statistical Mechanics*; HarperCollins Publisher, Inc.: New York, 1973. (b) Hill, T. L. *Statistical Thermodynamics*; Dover Publications, Inc.: New York, 1986.

(8) Süss-Fink, G.; Stanislas, S.; Shul'pin, G. B.; Nizova, G. V.; Stoeckli-Evans, H.; Neels, A.; Bobillier, C.; Claude, S. *J. Chem. Soc., Dalton Trans.* **1999**, 3169.

(9) Slebodnick, C.; Pecoraro, V. L. *Inorg. Chim. Acta* **1998**, *283*, 37.